

# Effects of $\tau_1$ Scattering on Fourier-Transformed Inelastic Tunneling Spectra in High- $T_c$ Cuprates with Bosonic Modes

Jian-Xin Zhu,<sup>1</sup> K. McElroy,<sup>2,3</sup> J. Lee,<sup>2</sup> T. P. Devereaux,<sup>4</sup> Qimiao Si,<sup>5</sup> J. C. Davis,<sup>2</sup> and A. V. Balatsky<sup>1</sup>

<sup>1</sup> *Theoretical Division, MS B262, Los Alamos National Laboratory, Los Alamos, New Mexico 87545, USA*

<sup>2</sup> *LASSP, Department of Physics, Cornell University, Ithaca, New York 14850, USA*

<sup>3</sup> *Department of Physics, University of California, Berkeley, California 94720-7300, USA*

<sup>4</sup> *Department of Physics, University of Waterloo, Ontario, Canada N2L 3G1 and*

<sup>5</sup> *Department of Physics & Astronomy, Rice University, Houston, Texas 77005, USA*

(Dated: June 21, 2005)

We study the  $\tau_1$ -impurity induced  $\mathbf{q}$ -space pattern of the energy derivative local density of states (LDOS) in a  $d$ -wave superconductor. We are motivated in part by the recent scanning tunneling microscopy (STM) observation of strong gap inhomogeneity with weak charge density variation in  $\text{Bi}_2\text{Sr}_2\text{CaCu}_2\text{O}_{8+\delta}$  (BSCCO). The hypothesis is that the gap inhomogeneity might be triggered by the disorder in pair potential. We focus on the effects of electron coupling to various bosonic modes, at the mode energy shifted by the  $d$ -wave superconducting gap. The pattern due to a highly anisotropic coupling of electrons to the  $B_{1g}$  phonon mode is similar to preliminary results from the Fourier transformed inelastic electron tunneling spectroscopy (FT-IETS) STM experiment in BSCCO. We discuss the implications of our results in the context of band renormalization effects seen in the ARPES experiments, and suggest means to further explore the electron-boson coupling in the high- $T_c$  cuprates.

PACS numbers: 74.25.Jb, 74.50.+r, 74.20.-z, 73.20.Hb

The extent to which collective excitations of high- $T_c$  cuprates are manifested in their single particle spectra is a long standing issue. The band renormalization effects, seen in the ARPES [1] (as well as in the break junction tunneling experiments [2]), have the characteristics of an electron-bosonic mode coupling. The “41 meV” spin resonance mode, a prominent feature in the spin excitation spectrum, is a natural candidate for electrons to couple to [3, 4, 5]. However, there are also phonon modes of similar energies, and they may instead have the strongest influence on the single electron spectra [6, 7, 8, 9]. At present, ARPES alone appears inadequate to differentiate the two scenarios. Sometime ago, several of us proposed [10] an FT-IETS STM technique as a complimentary means to study this issue. The technique takes advantage of the pioneering work of the Fourier transformed STM [11, 12], and combines it with the vintage IETS [13, 14, 15].

Central to this technique is the Fourier transform of the energy derivative of tunneling conductance map in real space  $d^2I/dV^2(\mathbf{r}, eV) \rightarrow d^2I/dV^2(\mathbf{q}, eV)$ . This  $\mathbf{q}$ -space map, which can also be called Fourier map, contains information about inelastic scattering in the system. Theoretically, one finds peaks in  $\mathbf{q}$  space and energy  $eV$  in this Fourier map of IETS that are related to the inelastic scattering off some collective excitations in the system. In the case of electron-spin mode coupling, the FT-LDOS near an ordinary potential scattering center (a  $\tau_3$  impurity in the Nambu space) at the energy of  $E = \pm(\Delta_0 + \Omega_0)$  was shown to have sharp features at momenta close to  $(\pi, \pi)$ . (Here  $\Delta_0$  is the maximum of the  $d$ -wave superconducting energy gap and  $\Omega_0$  the mode energy.)

Recently preliminary results from the first FT-IETS

STM experiment has been reported in BSCCO [16]. While features are observed in the Fourier-transformed  $d^2I/dV^2$  at the expected energy range, observed intensity near  $(\pi, \pi)$  is low. Instead, the strongest intensity appears at the wavevectors parallel to the Cu-O bond directions. These experimental results have in turn motivated us to compare the FT-IETS spectra near a potential scatterer in the cases of electrons coupled to the spin resonance and various phonon modes [17]. It was shown that all cases contain sharp features near  $(\pi, \pi)$ , in disagreement with the experimental spectrum.

This raises the question of whether the  $\tau_3$  scatterer correctly describes the impurities in  $\text{Bi}_2\text{Sr}_2\text{CaCu}_2\text{O}_{8+\delta}$  (BSCCO). The origin of ubiquitously observed nanoscale inhomogeneity in BSCCO has been investigated by studying the correlation between the inhomogeneity and the position of oxygen dopants [18]. It is shown that the local electronic states are not associated with charge density variations. To account for those features, Nunner *et al.* [19] proposed to look at the effect of random pairing potential fluctuations, the so-called  $\tau_1$  disorder. In what follows, we will address the effect of  $\tau_1$  disorder on FT-IETS signatures.

In this Letter, we take the disorder in pair potential as the scattering center, which is of  $\tau_1$  character in the Nambu space, and study the Fourier component of the energy derivative local density of states,  $d^2I/dV^2$ , at  $E \approx \pm(\Omega_0 + \Delta_0)$  around such a scatterer. We considered a few typical bosonic modes as a possible scattering modes that produce IETS fingerprints. We find that the results for  $\tau_1$  are qualitatively different from the case of potential disorder: 1) there are no strong signatures near in the  $\mathbf{q}$ -space near  $(\pi, \pi)$  in any of the electron-

boson couplings; 2) the highly anisotropic coupling of electrons to the out-of-plane out-of-phase oxygen buckling  $B_{1g}$  phonon mode, gives rise to a Fourier pattern similar to the IETS-STM experiment in BSCCO [16]. Our results are also consistent with the in-plane breathing mode although the agreement with the data is not as good.

We start with a model Hamiltonian for a two-dimensional  $d$ -wave superconductor with the coupling of electrons to bosonic modes:

$$\mathcal{H} = \mathcal{H}_{BCS} + \mathcal{H}_{el-boson} + \mathcal{H}_{imp}. \quad (1)$$

Here the bare BCS Hamiltonian,  $\mathcal{H}_{BCS} = \sum_{\mathbf{k}, \sigma} \xi_{\mathbf{k}} c_{\mathbf{k}\sigma}^\dagger c_{\mathbf{k}\sigma} + \sum_{\mathbf{k}} (\Delta_{\mathbf{k}} c_{\mathbf{k}\uparrow}^\dagger c_{-\mathbf{k}\downarrow}^\dagger + \Delta_{\mathbf{k}}^* c_{-\mathbf{k}\downarrow} c_{\mathbf{k}\uparrow})$ , where the normal state energy dispersion is given by [20],  $\xi_{\mathbf{k}} = -2t_1(\cos k_x + \cos k_y) - 4t_2 \cos k_x \cos k_y - 2t_3(\cos 2k_x + \cos 2k_y) - 4t_4(\cos 2k_x \cos k_y + \cos k_x \cos 2k_y) - 4t_5 \cos 2k_x \cos 2k_y - \mu$ , with  $t_1 = 1$ ,  $t_2 = -0.2749$ ,  $t_3 = 0.0872$ ,  $t_4 = 0.0938$ ,  $t_5 = -0.0857$ , and  $\mu = -0.8772$ , and the  $d$ -wave gap dispersion  $\Delta_{\mathbf{k}} = \frac{\Delta_0}{2}(\cos k_x - \cos k_y)$ . Unless specified explicitly, the energy is measured in units of  $t_1$  hereafter. The coupling of the electrons to bosonic modes is modeled by the Hamiltonian  $\mathcal{H}_{el-boson} = \frac{1}{\sqrt{N_L}} \sum_{\sigma} \sum_{\mathbf{k}, \mathbf{q}} g_{\nu}(\mathbf{k}, \mathbf{q}) c_{\mathbf{k}+\mathbf{q}, \sigma}^\dagger c_{\mathbf{k}\sigma} (b_{\nu\mathbf{q}} + b_{\nu, -\mathbf{q}}^\dagger)$  for the buckling  $B_{1g}$  ( $\nu = 1$ ) and the in-plane half breathing ( $\nu = 2$ ) modes, while  $\mathcal{H}_{el-boson} = \frac{g_0}{2N_L} \sum_{\sigma, \sigma'} \sum_{\mathbf{k}, \mathbf{q}} c_{\mathbf{k}+\mathbf{q}, \sigma}^\dagger (\mathbf{S}_{\mathbf{q}} \cdot \boldsymbol{\sigma}_{\sigma\sigma'}) c_{\mathbf{k}, \sigma'}$  for the spin resonance mode. For the phonon modes, we consider the cases where the coupling matrix element is either highly anisotropic, dependent on both  $\mathbf{k}$  and  $\mathbf{q}$ , or is only  $\mathbf{q}$  dependent. In the following we use the notation  $B_{1g}$ -I and  $br$ -I for the former type of phonon modes while  $B_{1g}$ -II and  $br$ -II for the latter type. Detailed expression of the coupling matrix elements for these types of phonon modes can be found in Ref. [17]. The third term describes the quasiparticles scattered off a  $\tau_1$  impurity due to the inhomogeneity in pair potential rather than off a conventional  $\tau_3$  impurity. In the following, we consider a single  $\tau_1$  impurity in a  $d$ -wave superconductor. The resulting Fourier pattern should survive a white-noise random distribution of such  $\tau_1$  impurities in a realistic system. The impurity part of Hamiltonian can then be written as:

$$\mathcal{H}_{imp} = \delta\Delta \sum_{\delta} \eta_{\delta} [c_{0\uparrow}^\dagger c_{\delta\downarrow}^\dagger + c_{\delta\uparrow}^\dagger c_{0\downarrow}^\dagger + H.c.], \quad (2)$$

where  $\eta_{\delta} = 1(-1)$  for  $\delta = \hat{x}(\hat{y})$ .

To be relevant to recent experimental realization, where no impurity-induced resonance state was observed, we assume the  $\tau_1$  impurity to have a weak scattering potential  $\delta\Delta$ . In this limit, we employ the Born approximation and arrive at the correction to the LDOS at the

$i$ -th site, summed over two spin components:

$$\delta\rho(\mathbf{r}_i, E) = -\frac{2\delta\Delta}{\pi} \sum_{\delta} \eta_{\delta} \text{Im}[\hat{\mathcal{G}}(i, 0; E+i\gamma) \hat{\tau}_1 \hat{\mathcal{G}}(\delta, i; E+i\gamma)]_{11}, \quad (3)$$

where  $\hat{\mathcal{G}}$  is the Green's function dressed with the bosonic renormalization effect and defined in the Nambu space [17]. From the perspective of the IETS, the energy derivative of the LDOS,  $\frac{d\delta\rho(\mathbf{r}_i, E)}{dE}$ , is the quantity we are most interested in. It corresponds to the derivative of the local differential tunneling conductance (i.e.,  $d^2I/dV^2$ ). The Fourier component of the differential LDOS is then given by  $\frac{d\delta\rho(\mathbf{q}, E)}{dE} = \sum_i \frac{d\delta\rho(\mathbf{r}_i, E)}{dE} e^{-i\mathbf{q}\cdot\mathbf{r}_i}$  with the spectral weight defined as  $P(\mathbf{q}, E) = \left| \frac{d\delta\rho(\mathbf{q}, E)}{dE} \right|$ .

We consider here for comparison the coupling of electrons to spin resonance mode,  $B_{1g}$  and breathing phonon modes. For the numerical calculation, we take the superconducting energy gap  $\Delta_0 = 0.1$ , the frequency of all bosonic modes  $\Omega_0 = 0.15$ . The  $\tau_1$  impurity scattering strength  $\delta\Delta$  is taken to be 50% of the superconducting energy gap. The coupling strength for all types of bosonic modes is calibrated to give at the Fermi energy  $E = 0$  an identical frequency renormalization factor in the self energy. The same procedure as in Ref. [17] is followed to obtain the Fourier spectral weight  $P(\mathbf{q}, E)$ .

In Figs. 1, we present the results of the Fourier spectrum,  $P(\mathbf{q}, E)$ , at the energy  $E = -(\Delta_0 + \Omega_0)$  for a  $d$ -wave superconductor with the electronic coupling to the bosonic modes. For comparison, the same spectrum is also shown (last panel) for the case of no mode coupling. Note that the case without the mode coupling, the energy  $\Omega_0$  has no special meaning in the context of the electronic properties, and the energy  $E = -(\Delta_0 + \Omega_0)$  is chosen merely for comparison to the case of mode coupling. The energy  $E = -(\Delta_0 + \Omega_0)$  corresponds to the position where the bosonic modes are excited, signaling a peak in the IETS  $d^2I/dV^2$ - $V$  tunneling spectrum [17]. First of all, the Fourier maps for all cases does not display any peak structure at large  $\mathbf{q}$  near  $(\pm\pi, \pm\pi)$  and  $(\pm\pi, \mp\pi)$ , which appears persistently with the  $\tau_3$  scattering [17]. Instead the Fourier spectral weight is minimal in intensity (dark blue area in the figure) in these regions. The map for the case of electronic coupling to the  $B_{1g}$ -I phonon mode shows locally strongest intensity (red spots) at  $\mathbf{q}$  about  $(\pm\frac{2\pi}{4}, 0)$  and  $(0, \pm\frac{2\pi}{4})$ . The peak intensity at  $\mathbf{q}$  near  $(\pm\frac{2\pi}{4}, \pm\frac{2\pi}{4})$  and  $(\pm\frac{2\pi}{4}, \mp\frac{2\pi}{4})$  is much weaker than those along the bond directions. The map for the case of the coupling to the  $br$ -I phonon mode exhibits locally strongest intensity (red spots) at  $\mathbf{q}$  near  $(\pm\frac{3\pi}{10}, 0)$  and  $(0, \pm\frac{3\pi}{10})$ . In addition, each of these red spot has a double-tail structure, which is absent in the case of  $B_{1g}$ -I mode coupling. The maps for the cases of the  $B_{1g}$ -II and spin resonance mode coupling exhibit similar  $\mathbf{q}$  structure. The finite intensity is uniformly distributed on a circular strip near  $|\mathbf{q}| = \frac{2\pi}{4}$  and becomes

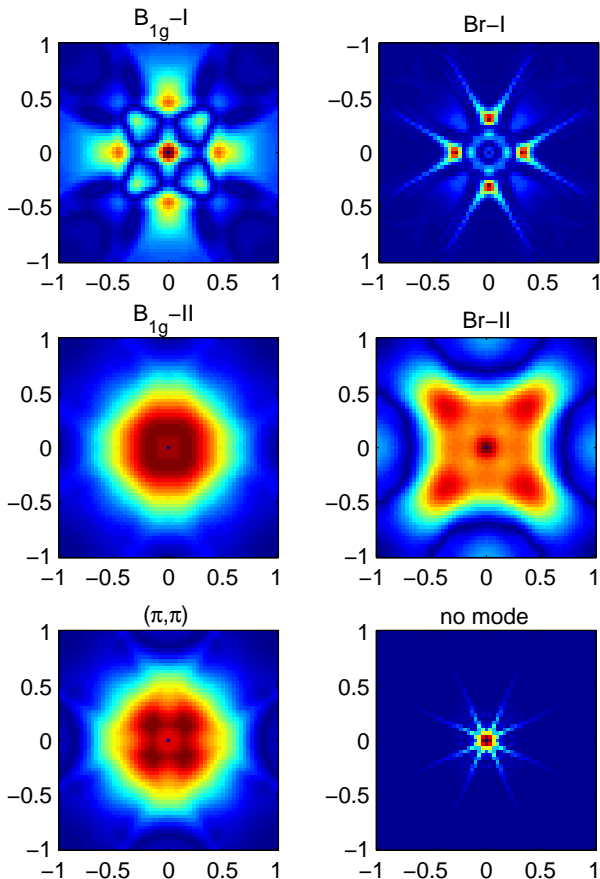


FIG. 1: The Fourier spectrum of the energy derivative LDOS at the energy  $E = -(\Delta_0 + \Omega_0)$  for a  $d$ -wave superconductor with the electronic coupling to the  $B_{1g}$ -I,  $br$ -I,  $B_{1g}$ -II,  $br$ -II, spin resonance modes. For comparison, the spectrum is also shown for the case of no mode coupling.

stronger as  $\mathbf{q}$  approaches the zero point. No locally distinguishable strongest intensity peak can be identified at  $\mathbf{q} = (\pm\frac{2\pi}{4}, 0)$  and  $(0, \pm\frac{2\pi}{4})$ . The map for the coupling to the  $br$ -II phonon mode exhibits locally the highest intensity (red spots) at  $\mathbf{q}$  near  $(\pm\frac{2\pi}{4}, \pm\frac{2\pi}{4})$  and  $(\pm\frac{2\pi}{4}, \mp\frac{2\pi}{4})$ . No peaks are found at  $\mathbf{q}$  near  $(\pm\frac{2\pi}{4}, 0)$  and  $(0, \pm\frac{2\pi}{4})$ . The map for the case of no mode coupling shows an eight-tail star shape at  $\mathbf{q} = (0, 0)$ , which consists of the head-on overlap of four red spots, such as those appearing in the case of the  $br$ -I phonon mode coupling each with two tails. As we have already emphasized, experimentally, the Fourier map of  $d^2I/dV^2$  shows intensity peaks only at  $\mathbf{q} = (\pm\frac{2\pi}{5}, 0) \pm 15\%$  and  $(0, \pm\frac{2\pi}{5}) \pm 15\%$  [16]. Therefore, by comparison with the experimental data, our new FT-IETS STM analysis also supports the notion [2, 3, 4, 5, 6, 7, 8, 9] that the electronic band must be renormalized by its coupling to the bosonic modes. In particular, the results based on the scenario of highly anisotropic coupling of electrons to the  $B_{1g}$  phonon mode are in best agreement with the IETS-STM data in BSCCO.

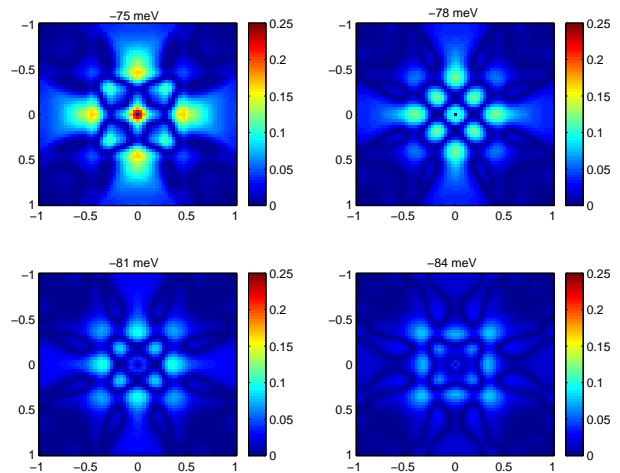


FIG. 2: The Fourier spectrum of the derivative of the LDOS is shown at the various values of the energy for the case of the electronic coupling to the  $B_{1g}$ -I phonon mode. Here the energy has been measured by scaling  $\Delta_0 = 30$  meV.

In Fig. 2, we present the energy evolution Fourier pattern for the electronic coupling to the  $B_{1g}$ -I mode. It shows that the intensity peak structure along the bond direction is robust against the energy change. The characteristic  $q$  vector, at which the locally highest intensity is located, decreases slightly with the increased energy. This result is also not inconsistent with the preliminary experiment.

Our results demonstrate the important role the character of the scattering center plays in the Fourier spectrum. To explore this issue further, we note that, in the case of  $\tau_1$  scattering considered here, the Fourier spectrum can be expressed as follows,

$$\begin{aligned} \delta\rho(\mathbf{q}; E) = & \frac{2\delta\Delta}{N_L} \sum_{\mathbf{k}} (\cos k_x - \cos k_y) \\ & \times \{ [A(\mathbf{k}; E)K(\mathbf{k} + \mathbf{q}; E) + K(\mathbf{k}; E)A(\mathbf{k} + \mathbf{q}; E)] \\ & + [J(\mathbf{k}; E)B(\mathbf{k} + \mathbf{q}; E) + B(\mathbf{k}; E)J(\mathbf{k} + \mathbf{q}; E)] \}, \quad (4) \end{aligned}$$

where

$$A(\mathbf{k}; E) = -\frac{2}{\pi} \text{Im}[\mathcal{G}_{11}(\mathbf{k}; E + i\gamma)], \quad (5)$$

$$B(\mathbf{k}; E) = \text{Re}[\mathcal{G}_{11}(\mathbf{k}; E + i\gamma)], \quad (6)$$

$$J(\mathbf{k}; E) = -\frac{2}{\pi} \text{Im}[\mathcal{G}_{12}(\mathbf{k}; E + i\gamma)], \quad (7)$$

$$K(\mathbf{k}; E) = \text{Re}[\mathcal{G}_{12}(\mathbf{k}; E + i\gamma)]. \quad (8)$$

This expression shows that, for the  $\tau_1$  scattering, the Fourier spectrum is determined by the  $\mathbf{k}$ -summation of the product terms constituting the imaginary (real) parts of the single-particle ( $\mathcal{G}_{11}$ ) with the real (imaginary) parts of anomalous ( $\mathcal{G}_{12}$ ) Green's function in the superconducting state, *weighted by a  $d$ -wave type form factor*  $\cos k_x - \cos k_y$ . This scattering process with the  $\tau_1$  impurity is significantly different than the case of a

$\tau_3$  impurity scattering [17], where the convolution takes place between the real and imaginary parts of the same Green's function without the form factor. This difference of the scattering process matters significantly in the resulting Fourier map. As shown in Eq. (4), the form factor  $\cos k_x - \cos k_y$  appearing in the  $\tau_1$  scattering case is identically zero along the diagonals in the first Brillouin, but reaches a maximum at the  $M$  points [ $\mathbf{k} = (\pm\pi, 0)$  and  $(0, \pm\pi)$ ] on the zone boundary. It then follows that any stronger intensity from the product of  $AK$ ,  $BJ$  connected by a  $\mathbf{q}$  oriented close to the diagonals is strongly suppressed, while the intensity connected by  $\mathbf{q}$  oriented parallel to the bond direction is enhanced. For the electronic coupling to the  $B_{1g}$ -I phonon mode, it has been found [17] that there are moderately strong intensity on the two split beams oriented perpendicular to the zone boundary at  $M$  points in the function  $A$ ,  $B$ ,  $J$ , and  $K$ . The form factor  $\cos k_x - \cos k_y$  then tips the relative contribution from the product  $AK$  and  $BJ$ , giving rise to locally highest intensity at  $\mathbf{q} = (\pm\frac{2\pi}{4}, 0)$  and  $(0, \pm\frac{2\pi}{4})$  in the Fourier map (see the first panel of Fig. 1). These split beams of intensity are absent for the electronic coupling to other modes.

Our results naturally suggest additional means to further explore the electron-bosonic mode coupling experimentally. For instance, a Zn impurity acts as a non-magnetic potential center – a  $\tau_3$  scatterer. In this case, the sharp features near  $(\pi, \pi)$  should be observed in the FT-IETS spectrum. In the case of low-energy elastic scattering interference of quasiparticles, related effects have in fact been demonstrated. Indeed, strong signatures near  $(\pm\pi, \pm\pi)$  and  $(\pm\pi, \mp\pi)$  appear in the theoretical spectra near a  $\tau_3$  scatterer [21]. These features are not observed experimentally in the stoichiometrical BSCCO [11, 12], but are seen around a nonmagnetic Zn impurity in the doped BSCCO.

In conclusion, we have studied, for the first time, the  $\tau_1$ -impurity induced Fourier pattern of the energy derivative local density of states in a  $d$ -wave superconductor with the coupling of electrons to various bosonic modes. We consider  $B_{1g}$ , half-breathing, and spin  $(\pi, \pi)$  modes. Our results show that, at the mode energy shifted by the  $d$ -wave superconducting gap energy  $\Delta_0$ , i.e.,  $E = \pm(\Delta_0 + \Omega_0)$ , the coupling of electrons to the  $B_{1g}$  or breathing phonon modes, gives rise to a Fourier pattern similar to the preliminary Fourier transformed IETS-STM experiment in BSCCO [16]. The coupling of electrons to the spin resonance mode, on the other hand, yields a Fourier spectrum that is inconsistent with the experiment. These results do not necessarily rule out the role of the spin-spin interactions as being relevant for superconductivity in BSCCO, instead they imply that electron-phonon coupling has a strong impact on the superconducting electronic structure. These results have important implications for our understanding of the electronic properties of the cuprates. They also demonstrate

the potential of the FT-IETS STM technique, and highlight the importance of  $\tau_1$  scattering in the impurity-free BSCCO [19].

We thank D.-H. Lee, N. Nagaosa, M. R. Norman, D. J. Scalapino, and Z. X. Shen for very useful discussions. This work was supported by the US DOE (J.X.Z. and A.V.B.), the NSERC, the Office of Naval Research under Grant No. N00014-05-1-0127, and the A. von Humboldt Foundation (T.P.D.), the NSF under Grant No. DMR-0424125 and the Robert A. Welch Foundation (Q.S.), the Office of Naval Research under grant N00014-03-1-0674, the NSF under Grant No. DMR-9971502, the NSF-ITR FDP-0205641, and the Army Research Office under Grant No. DAAD19-02-1-0043 (K.M., J.L., and J.C.D.).

- 
- [1] A. Damascelli, Z. Hussain, and Z.-X. Shen, *Rev. Mod. Phys.* **75**, 473 (2003), and references therein.
  - [2] J. F. Zasadzinski, L. Ozyuzer, N. Miyakawa, K. E. Gray, D. G. Hinks, and C. Kendziora, *Phys. Rev. Lett.* **87**, 067005 (2001), and references therein.
  - [3] M. R. Norman, M. Eschrig, A. Kaminski, and J. C. Campuzano, *Phys. Rev. B* **64**, 184508 (2001); M. R. Norman and H. Ding, *Phys. Rev. B* **57**, 11089 (1998).
  - [4] Ar. Abanov and A. V. Chubukov, *Phys. Rev. Lett.* **83**, 1652 (1999).
  - [5] M. Eschrig and M. R. Norman, *Phys. Rev. Lett.* **85**, 3261 (2000).
  - [6] A. Lanzara, P. V. Bogdanov, X. J. Zhou, S. A. Kellar, D. L. Feng, E. D. Lu, T. Yoshida, H. Eisaki, A. Fujimori, K. Kishio, J.-I. Shimoyama, T. Noda, S. Uchida, Z. Hussain, Z.-X. Shen, *Nature* **412**, 510 (2001).
  - [7] T. Cuk, F. Baumberger, D. H. Lu, N. Ingle, X. J. Zhou, H. Eisaki, N. Kaneko, Z. Hussain, T. P. Devereaux, N. Nagaosa, and Z.-X. Shen, *Phys. Rev. Lett.* **93**, 117003 (2004).
  - [8] A. W. Sandvik, D. J. Scalapino, and N. E. Bickers, *Phys. Rev. B* **69**, 094523 (2004).
  - [9] T. P. Devereaux, T. Cuk, Z.-X. Shen, and N. Nagaosa, *Phys. Rev. Lett.* **93**, 117004 (2004).
  - [10] J.-X. Zhu, J. Sun, Q. Si, and A. V. Balatsky, *Phys. Rev. Lett.* **92**, 017002 (2004).
  - [11] J. E. Hoffman, K. McElroy, D.-H. Lee, K. M. Lang, H. Eisaki, S. Uchida, and J. C. Davis, *Science* **297**, 1148 (2002).
  - [12] K. McElroy, R. W. Simmonds, J. E. Hoffman, D. H. Lee, J. Orenstein, H. Eisaki, S. Uchida, J. C. Davis, *Nature* **422**, 592 (2003).
  - [13] R.C. Jaklevic and J. Lambe, *Phys. Rev. Lett.* **17**, 1139 (1966).
  - [14] D.J. Scalapino and S.M. Markus, *Phys. Rev. Lett.* **18**, 459 (1967).
  - [15] A.V. Balatsky, Ar. Abanov, and J.-X. Zhu, *Phys. Rev. B* **68**, 214506 (2003).
  - [16] J. Lee, K. McElroy, J. Slezak, S. Uchida, H. Eisaki, and J.C. Davis, *Bull. Am. Phys. Soc.* **50**, 299, (2005); J.C. Davis, J. Lee, K. McElroy, J. Slezak, H. Eisaki, and S. Uchida, *Bull. Am. Phys. Soc.* **50**, p1223, (2005), J. Lee *et al*, unpublished.

- [17] J.-X. Zhu *et al.*, cond-mat/0507610 (unpublished).
- [18] K. McElroy *et al.*, to appear in Science.
- [19] T. S. Nunner, B. M. Anderson, A. Melikyan, and P. J. Hirschfeld, cond-mat/0504693 (unpublished).
- [20] M. R. Norman, M. Randeria, H. Ding, and J. C. Cam-  
puzano, Phys. Rev. B **52**, 615 (1995).
- [21] Q.-H. Wang and D.-H. Lee, Phys. Rev. B **67**, 020511  
(2003).